

Toningenieursprojekt

A Compact Spherical 170 Loudspeaker Array for Outdoors

Benedikt Brands

Supervisor:
Ass.Prof. DI Dr.rer.nat. Franz Zotter

Graz, November 29, 2022



institut für elektronische musik und akustik



Abstract

Die Fähigkeit, mit kompakten sphärischen Lautsprecherarrays fokussierte Schallstrahlen in ihrer Abstrahlrichtung steuern zu können, macht sie zu interessanten Werkzeugen für elektroakustische Kompositionen, die mit verräumlichtem Klang arbeiten. Alternativ zum aufwendigen Design des 20-kanaligen IKO wurden kleinere Modelle, wie das 393 Lautsprecherarray (15 Kanäle) oder das 170 Lautsprecherarray (8 Kanäle) für kleinere Performances, Proben und als leistbare persönliche Instrumente entwickelt. Die Anwendung davon ist nicht nur für Innenräume interessant, jedoch ergeben sich für Außenanwendungen erhöhte Anforderungen an Lautsprecher und Abdichtung: sie müssen Sonnenlicht, Feuchtigkeit und Regen standhalten, besonders bei Installationen, die über mehrere Tage laufen sollen. In diesem Projekt wird solch ein wetterfestes Lautsprecherarraydesign als Weiterentwicklung des 170 Arrays entworfen, gebaut und getestet. Zudem soll die Erweiterung um einen Tieftonlautsprecher und die dadurch mögliche Verbesserung der horizontalen Fokussierung messungsbasiert simuliert und diskutiert werden.

Compact spherical loudspeaker arrays are useful devices to produce focused beams of sounds with controllable radiation direction and hereby offer interesting means of expression in electroacoustic music, especially for spatialized sound. As alternative to the elaborate and expensive designs of the 20-channel IKO, small-scale models such as the 393 loudspeaker array (15 channels) or the 170 loudspeaker array (8 channels) were designed and built for small spaces, rehearsals, or to be affordable private instruments. The utilization of loudspeaker arrays needs not to be restricted to indoor performances, however, outdoor applications may require weatherproof designs, regarding sunlight, moisture, and rain in particular with installations that are supposed to be operating for several days. In this project such a weatherproof design will be conceptualized, built and tested on the basis of the existing 170 design. Moreover, the extension by one bass loudspeaker will be simulated to find out whether a 171 design is superior in terms of maintaining a horizontal focus.

Contents

1	Introduction	4
2	Design and Construction	5
3	Filter Design	7
3.1	Crosstalk-Cancellation-Filters (CTC)	7
3.2	Spherical-Harmonic (SH) Beamforming	10
3.3	Radiation Control	11
3.4	On-Axis Equalization	12
4	Directivity Measurement	14
5	Simulating a 171 design	16
6	Conclusion and Outlook	17



Figure 1 – The 170 loudspeaker array on site as part of an installation at Norges Hjemmefrontmuseum, Oslo (Courtesy of Natasha Barrett).

1 Introduction

A way to make spherical loudspeaker arrays for surround-sound reinforcement more accessible is to limit the number of transducers. As a drawback the designer would have to accept a diminished beamforming order, however the nature of the human hearing makes spatial information above and below the horizon negligible, hence a design with a horizontal ring of loudspeakers and optional elevated ones is a promising attempt for maintaining high-order beamforming with fewer channels.

Meyer-Kahlen et al. have built a cuboid loudspeaker array with only 4 drivers on the horizon enabling 1st-order beamforming [MKZP18]. Riedel's 393 prototype uses 9 horizontal and two elevated rings of 3 loudspeakers each, supporting 4th-order beamforming [RZ20], however its configuration still needs 15 separately amplified channels. The newest approach of the 170 prototype by Drack [DZB20] which, with 7 horizontal and one vertical speaker is capable of 3rd-order beamforming, will be used as basis in this project.

The above mentioned loudspeaker arrays were designed for indoor usage, however the artist may want to perform an installation outdoors. In such case, the design has to withstand environmental influences such as high humidity, UV-radiation and rain over a long time.

This work describes the construction of such a new weatherproof prototype, its filter design and measurement. An evaluation of the beamforming behavior is made and furthermore a short simulation is conducted to show a perspective on a thinkable 171 design.

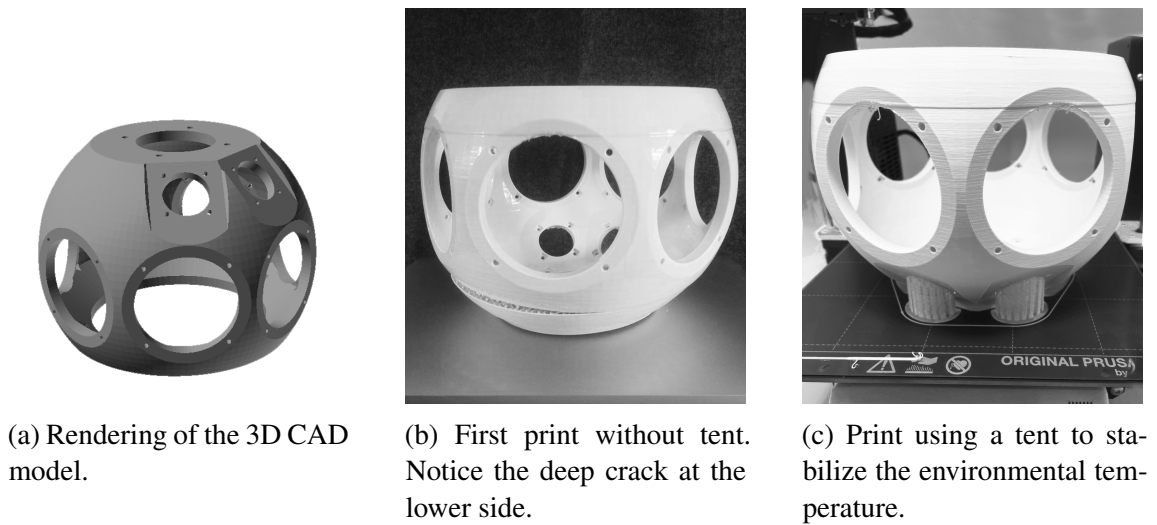


Figure 2 – 3D Rendering and printing steps of the prototype

2 Design and Construction

Following the design of the preceding prototype 170 loudspeaker array [DZB20] a ring of seven broadband transducers (Visaton FR-8 WP 3.3")¹ and one vertically mounted broadband sub-loudspeaker (Visaton FR-16 8")² were used. The manufacturer guarantees absolute corrosion-resistance and waterproofness due to encased magnet and silicon-coated leads, functionality at low temperatures and seawaterproofness. The speaker is also built with a grille to protect the membrane from impacts.

For two-dimensional layouts, the number of speakers n_h limit the maximum directivity order [Dan00]:

$$N_{max,2D} \leq \frac{(n_h - 1)}{2}, \quad (1)$$

hence this design enables third-order horizontal ambisonic beamforming. The 3D CAD model is depicted in Figure 2a.

Parts

All components have to withstand environmental influences such as rain, temperature changes and UV radiation. We chose to use fullrange speakers by Visaton which cones, baskets and grilles are made of ASA plastic and meet these requirements. Furthermore, all junctions from components (such as mounting flange and cable connectors) to the housing were sealed using a gasket and silicone.

1. <https://www.visaton.de/en/products/drivers/fullrange-systems/fr-8-wp-4-ohm-white>

2. <https://www.visaton.de/en/products/drivers/fullrange-systems/fr-16-wp-4-ohm-white>

Printing the Housing

We used a weatherproof ASA filament and a 3D printer by Prusa³ to print the prototype housing. Printing with ASA can be quite challenging since the thermoplastic is very sensitive to temperature changes during the printing process and reacts with warping, cf. Figure 2b. An approved method is to place the printer in a housing, for instance a photo studio shooting tent. This will maintain a relatively stable micro climate during the process and counters the material's tendency to warp. We also tried out adding printing supports at overhangs and in the speaker's slots but couldn't notice any benefit. Due to the relatively new printing technique and since it is mainly documented in online-forums and posts, the printing process was quite experimental and used a lot of trial-and-error. After several test prints a model of satisfactory quality could be crafted (Figure 2c) and a few slits that still occurred because of warping were sealed with silicone. The final assembled prototype is depicted in Figure 1 where it is installed in a hanging position with the horizontal speaker facing to the floor.

3. <https://www.prusa3d.com/product/original-prusa-i3-mk3s-3d-printer-3/>

3 Filter Design

To drive the loudspeaker array, an ambisonics-format input has to run through four blocks of signal processing, cf. Figure 3:

- Spherical-Harmonic (SH) Beamforming
- Radiation Control
- Crosstalk-Cancellation-Filters (CTC)
- On-Axis Equalization

These processing steps are described below and follow the method of Zotter et. al, who conceived them for the Icosahedral loudspeaker array [ZZFK17] and Riedel and Zotter, who explained them in detail for mixed-order compact spherical loudspeaker arrays, such as the 393 array [RZ20].

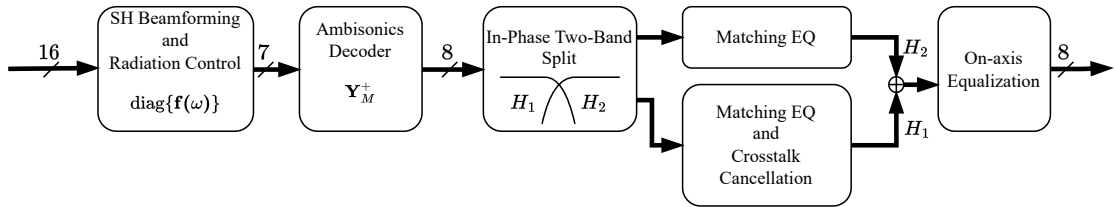


Figure 3 – Control block diagram for the 170 prototype with $L = 8$, $(N + 1)^2 = 16$ and 7 controlled harmonics

3.1 Crosstalk-Cancellation-Filters (CTC)

Since all loudspeakers are built into a common housing they are acoustically coupled by the air enclosed, and driving one loudspeaker actively with an input voltage will lead to passive movements of every other loudspeaker. To identify this crosstalk, velocities were measured using a laser Doppler vibrometer and the exponential sine-sweep method, cf. Figure 4. The laser beam had to be aimed exactly through one of the holes of the grille to give satisfactory results.

The multiple-input-multiple-output (MIMO) voltage-to-velocity transfer functions from the 8 loudspeaker to 8 on-axis laser vibrometry locations relate the input voltages $\mathbf{u}(\omega)$ to the output velocities $\mathbf{v}(\omega)$. Subsequent formulations hold for the frequency domain, and for brevity the notation of frequency dependency is omitted

$$\mathbf{v} = \mathbf{T}\mathbf{u}.$$

(2)



Figure 4 – Setup for the velocity measurement.

To obtain a system without crosstalk and with a flat magnitude response, a full system inversion \mathbf{T}^{-1} could be conducted. The disadvantage of this procedure is that it could lead to anti-causal components and infeasible long impulse responses. A more practical method obtains stable and short filters by designing a matched target response H_{mean} for the active paths that can be reached by equalizing the system matrix \mathbf{T} [RZ20]:

$$\mathbf{T}_{eqd} = \mathbf{T} \text{diag}\{\mathbf{h}_{eq}\} = H_{mean} \mathbf{I} + \mathbf{T}_{eqd,passive}. \quad (3)$$

This target H_{mean} is the third-octave-smoothed minimum-phase mean of the active paths of all loudspeaker responses and there it is easily inverted.

Since crosstalk decreases at high frequencies and to regularize the inversion effort at low frequencies, the measurements for the passive paths are treated with a zero-phase 4th-order bandpass filter ($f_1 = 100$ Hz, $f_2 = 2.5$ kHz), so crosstalk cancellation is only applied to meaningful frequencies. We get the modified MIMO-system

$$\tilde{\mathbf{T}}_{eqd} = H_{mean} \mathbf{I} + \mathbf{T}_{eqd,passive} H_{BP} \quad (4)$$

that is accordingly prepared, regularized and temporally well-behaved for inversion.

Finally, we arrive at the matching and crosstalk-cancelling system \mathbf{X}_c

$$\mathbf{X}_c = \text{diag}\{\mathbf{h}_{eq}\} \tilde{\mathbf{T}}_{eqd}^{-1} H_{mean}. \quad (5)$$

Cancellation performance

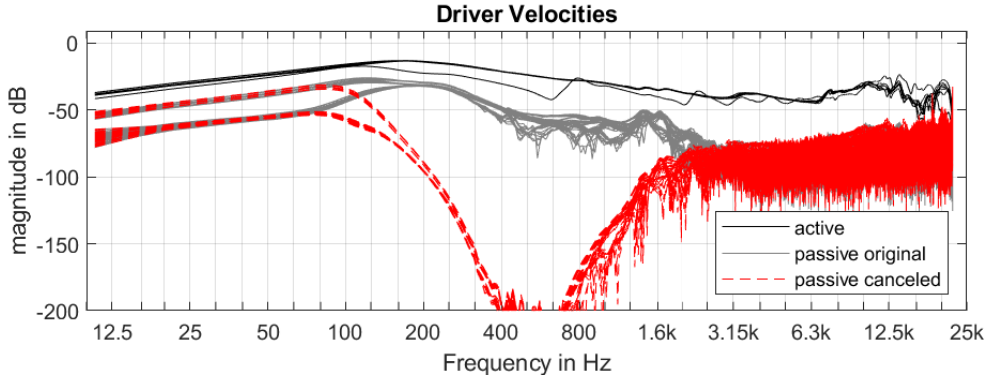


Figure 5 – Velocities of original versus canceled paths.

Figure 5 shows the magnitude responses of the active and original versus canceled passive coupling paths. At high frequencies the measurement becomes noisy due to partial vibrations and diffraction. Notice that below the loudspeaker's resonance frequencies ($f_{res,1} = 85$ Hz, $f_{res,2..8} = 158$ Hz) the passive paths from vertical to horizontal loudspeakers are about 20 dB stronger than vice versa. This can be explained by the different membrane area sizes. The vertical transducer with twice the radius than the horizontal ones can drive the passive paths more easily than vice versa.

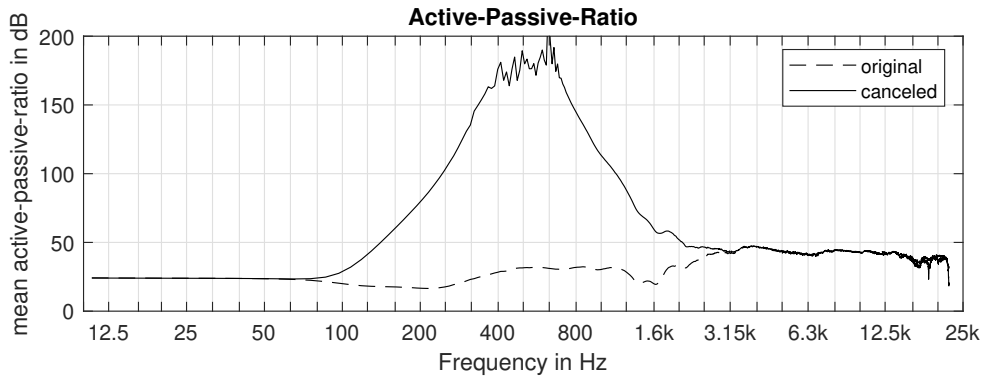


Figure 6 – Ratio of velocities of active to passive paths, averaged over all active, resp. passive paths.

As depicted in Figure 6, the crosstalk cancelling performance is enhanced from 30 dB to 50 dB and up to complete decoupling within a frequency range of 100 Hz to 2.5 kHz. Hereby an independent control of all transducers which is necessary for beamforming is guaranteed.

Subwoofer Control

Since we are mainly interested in directivity resolution in the horizontal plane and since for sub-band frequencies diffraction makes SH beamforming irrelevant, we use a separate control for the subwoofer. With that in mind, we use a separate minimum phase target $H_{2...8,mean}$ for the horizontal loudspeaker ring and for the subwoofer $H_{1,mean}$ which can reach lower frequencies. The separate controls still have the CTC in common and as depicted in the signal flow chart in Figure 7, the subwoofer input drives the subwoofer actively and cancels the passive movements of the horizontal speakers and vice versa for the horizontal speakers.

The final CTC system \mathbf{X}_c is obtained by computing $\mathbf{X}_{c,sub}$ and $\mathbf{X}_{c,2...8}$ with Equation 5 and joining the first column of $\mathbf{X}_{c,sub}$ and all but the first columns of $\mathbf{X}_{c,2...8}$.

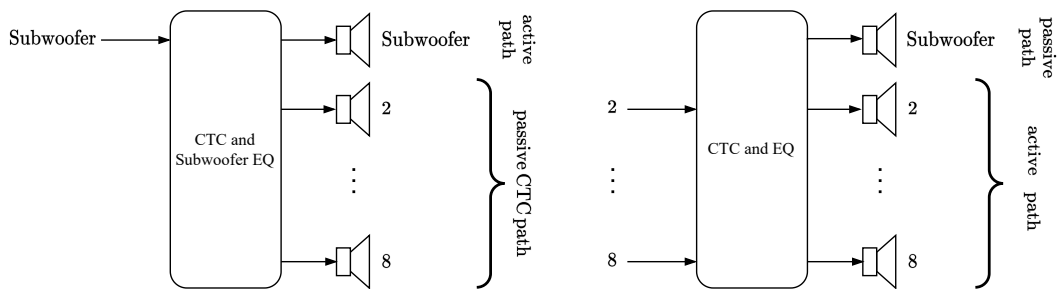


Figure 7 – Signal flow for the separate subwoofer and horizontal loudspeaker control.

In-Phase Two-Band Split

In the course of designing the CTC filters, an in-phase two-band split is designed with a crossover frequency of $f_c = 4$ kHz. This is done by using the square of a third-order butterworth low-pass and high-pass filter respectively and is described in detail by Lipshitz and Vanderkooy [LV86]. In the lower band, the processing utilizes the CTC and matching EQ, in the upper band, the inversion of complicated transducer responses is avoided and only the matching EQ is applied. For there still where problems regularizing the target responses at high frequencies, for every loudspeaker its third-octave smoothed measurement was used as a target and the averaging over all was discarded.

3.2 Spherical-Harmonic (SH) Beamforming

Directivity functions for spherical beamforming can be obtained by evaluating the spherical harmonics $Y_n^m(\boldsymbol{\theta})$ at the beam direction $\boldsymbol{\theta}_{beam}$ and the variable direction $\boldsymbol{\theta}$. Typically, the side lobes are suppressed by weights w_n

$$g(\boldsymbol{\theta}) = \mathbf{y}_N(\boldsymbol{\theta})^\top \text{diag}\{\tilde{\mathbf{w}}_N\} \mathbf{y}_N(\boldsymbol{\theta}_{beam}). \quad (6)$$

With

$$\begin{aligned} \mathbf{y}_N(\boldsymbol{\theta}) &= [Y_n^m(\boldsymbol{\theta})]_{n=0\dots N, m=-n\dots n}, \\ \tilde{\mathbf{w}}_N &= [w_n]_{n=0\dots N, m=-n\dots n}. \end{aligned} \quad (7)$$

Where w_n are the max- r_E weights approximated by Zotter and Frank [ZF12].

Mixed Order SH Beamforming

For mixed-order directivity patterns, a mask \mathbf{M} selects a subset of the spherical harmonics $Y_n^m(\boldsymbol{\theta})$ [RZ20]. For the 170 design, only the 7 SH's with degrees of freedom at the horizon are used, cf. Figure 8 and we obtain

$$\begin{aligned} g_M(\boldsymbol{\theta}) &= \mathbf{y}_N(\boldsymbol{\theta})^\top \mathbf{M}^\top \text{diag}\{\tilde{\mathbf{w}}_M\} \mathbf{M} \mathbf{y}_N(\boldsymbol{\theta}_{beam}) \\ &= \mathbf{y}_M(\boldsymbol{\theta})^\top \text{diag}\{\tilde{\mathbf{w}}_M\} \mathbf{y}_M(\boldsymbol{\theta}_{beam}) \end{aligned} \quad (8)$$

Where $\tilde{\mathbf{w}}_M = [\tilde{w}_{nm}^{(M)}]$ are the redefined weights that balance out for the omitted weights.

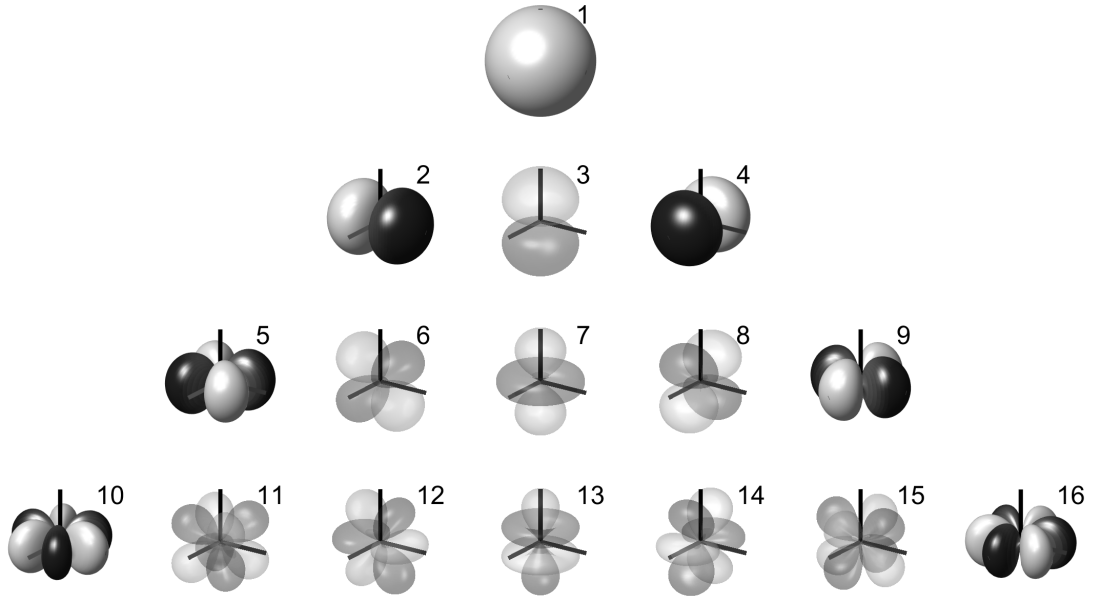


Figure 8 – Spherical harmonics up to order $N = 3$. Transparent plots depict the SH that are not included in the mixed-order subspace.

3.3 Radiation Control

Having selected the mixed-order subspace from the beampattern, we have to build the radiation control filters which include all necessary processing for the final transducer voltages.

Spherical Cap Model

To calculate the far-field sound pressure due to velocities on the surface of the rigid sphere, we use the spherical cap model as proposed by Zotter et. al in matrix form [ZSH07]:

$$p(\boldsymbol{\theta}) = \mathbf{y}(\boldsymbol{\theta})^\top \text{diag}\{\mathbf{h}(\omega)\} \text{diag}\{\mathbf{a}\} \mathbf{Y} \mathbf{v}, \quad (9)$$

with the real-valued spherical harmonics evaluated at the cap positions \mathbf{Y} , the cap coefficients \mathbf{a} and the propagator $h(\omega)$ that uses the derivative of the spherical Hankel function of the second kind h'_n :

$$\begin{aligned} \mathbf{Y} &= [\mathbf{y}(\boldsymbol{\theta}_1) \dots \mathbf{y}(\boldsymbol{\theta}_L)], \\ \mathbf{h}(\omega) &= \frac{i^n}{k h'_n(kR)}, \\ \mathbf{a} &= [a_n]_{n=0 \dots N, m=-n \dots n}, \end{aligned} \quad (10)$$

with

$$a_0 = 2\pi(1 - \cos \frac{\alpha}{2}), \text{ and}$$

$$a_n = 2\pi \frac{\cos \frac{\alpha}{2} P_n(\cos \frac{\alpha}{2}) - P_{n+1}(\cos \frac{\alpha}{2})}{n}, \text{ for } n > 0.$$

With the weighted desired beam pattern as input for the inverse propagator, inverse cap coefficients and pseudoinverse rectangular matrix \mathbf{Y}_M^+ of the cap positions, all in mixed-order subspace, we obtain the cap velocities \mathbf{v} for further treatment

$$\mathbf{v} = \mathbf{Y}_M^+ \text{diag}\{\mathbf{a}_M\}^{-1} \text{diag}\{\mathbf{h}_M(\omega)\}^{-1} \text{diag}\{\tilde{\mathbf{w}}_M\} \mathbf{y}_M(\boldsymbol{\theta}_{beam}). \quad (11)$$

Radial Filters

To meet the physical limitations of loudspeakers a regularization of the inverse propagator is required since the formal results would yield radial far-field filters with drastically increasing magnitudes towards low frequencies. The limitation is realized with an equal-phase filter bank $B_b(\omega)$ with one bank b per ambisonics order $n = 0 \dots N$, as described by Frank and Zotter [ZZFK17]. In practice, the cutoff frequencies are chosen such that the excursions of the loudspeakers do not exceed a certain value for all bands. The cutoff frequencies for the 170 prototype are listed in Table 1.

	f_1	f_2	f_3	f_4
Hz	145	226	315	461

Table 1 – Cutoff frequencies for Radiation Control filter bank

Radiation control $g(\omega)$ now includes the limited radial filters, the weighting, the inverse propagator and cap coefficients

$$\mathbf{g}(\omega) = \left[\frac{kh'_n(kR)}{i^n a_n} \sum_{b=n}^N B_b(\omega) w_{nm}^{(b)} e^{ikR} \right]_{n,m \in M}, \quad (12)$$

which together with the decoder \mathbf{Y}_M^+ map the desired beam pattern to the cap velocities

$$\mathbf{v} = \mathbf{Y}_M^+ \text{diag}\{\mathbf{g}(\omega)\} \mathbf{y}_M(\boldsymbol{\theta}_{beam}). \quad (13)$$

3.4 On-Axis Equalization

The frequency response of the whole system, including the interaction with the acoustic environment, is of great importance for the final quality. We made a measurement with the loudspeaker array placed within a studio room and measured the response of a beam pointed towards the microphone at approximately 1.5 m distance and used an equalizer to meet the target response within tolerance bounds. The client decided to use an averaged

measurement over all loudspeakers at minimum distance since the installation took place in an outside yard of a castle with less prominent room response. Both filter curves are depicted in Figure 9.

All software used hereafter is freely available and downloadable via the links. For the measurement, Room Equalization Wizard (REW)⁴ was used. In the software, the third-octave-smoothed curve was treated with parametric equalizers to fulfill the bounds of a target curve. The EQ parameters were then copied to an instance of the VST-plugin `mcfx_filter` from the `mcfx` plug-in suite⁵ located in the DAW Reaper⁶. Now, the target response could be reviewed by routing the sweep output from REW throughout the equalizer in Reaper and the microphone input back again into REW. After verification, the filter curve was implemented as an impulse response with $N = 2049$ sampling points at a sampling frequency of $f_s = 44.1$ kHz for usage with a simple convolver plugin, for instance the `mcfx_convolver`⁵.

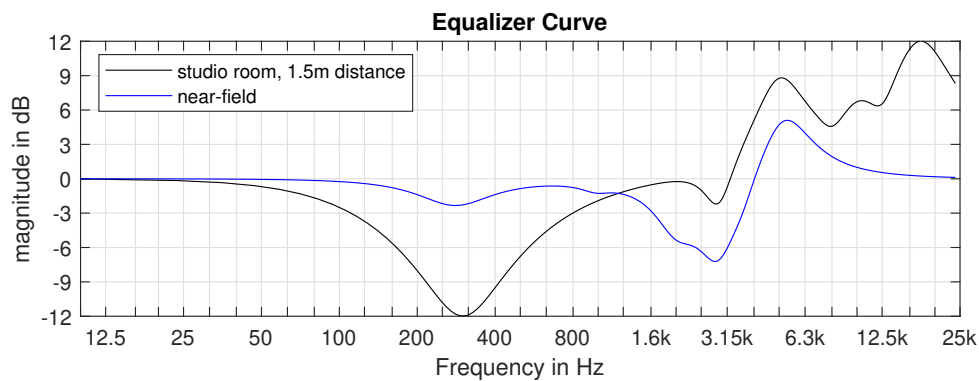


Figure 9 – The two filter curves for overall equalization

4. <https://www.roomeqwizard.com/>

5. <https://github.com/kronihias/mcfx>

6. <https://www.reaper.fm/>

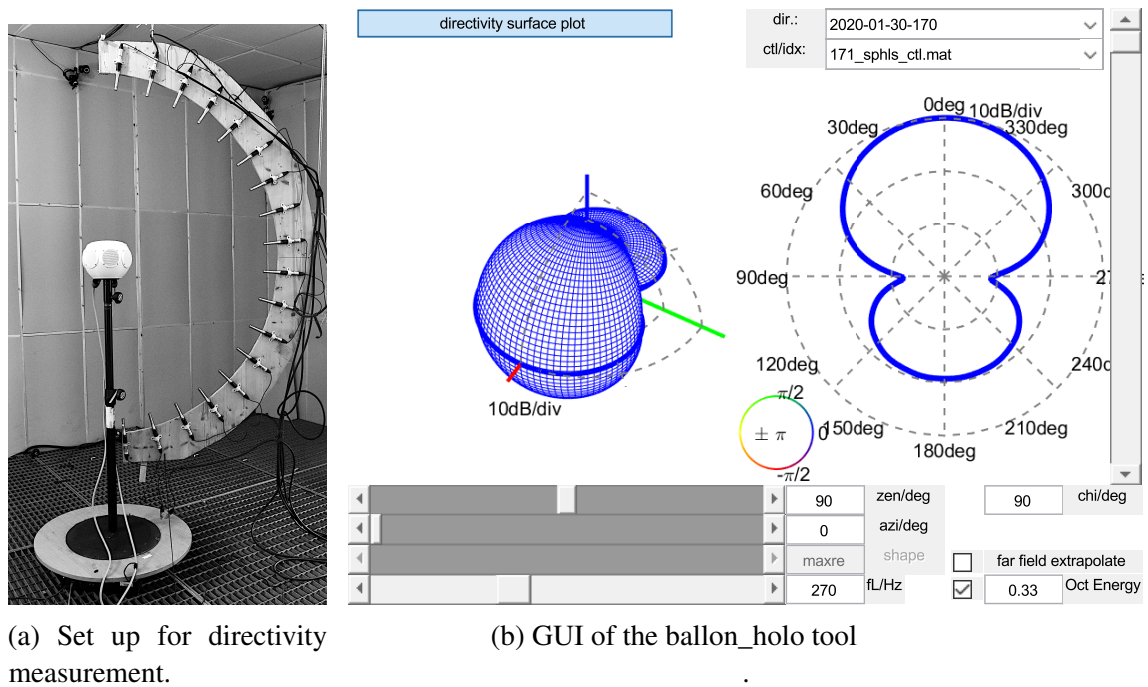


Figure 10

4 Directivity Measurement

For measuring the directivity patterns of a spherical loudspeaker array, the existing routine was used and the sound pressures at radius $r = 77.5$ cm were captured at a resolution of 10° for azimuth and elevation. The measurement was conducted in the anechoic chamber at IEM. The setup consisted of 18 microphones that were attached to a semicircle, and a rotary plate was used to turn the loudspeaker array. The setup is depicted in Figure 10a.

The total of $8 \cdot 18 \cdot 36 = 5184$ impulse responses were then stored in the SOFA format⁷ and, together with the control filters, fed to the open source tool `ballon_holo` which is capable of visualizing the directivity behavior in terms of 3D polar diagrams, cf. Figure 10b and directivity surface (Figure 11-12)

As expected, the 170 loudspeaker array performs less vertical focusing as horizontal. We can observe a stable beam with less than 15 dB sound pressure loss in an angle of $\pm 30^\circ$ for horizontal versus $\pm 90^\circ$ for vertical beamforming over a frequency range of 400 Hz–6 kHz. Due to diffraction at low frequencies and the small radius of the housing, beamforming starts at 250 Hz. At 1.2 kHz spatial aliasing starts disturbing the focusing and comb filter cancellation effects are visible above 8 kHz upwards. For the vertical cut similar disturbance behavior appears and, moreover, floor reflections appear as cancellation patterns within the lower half of the plot.

7. <https://www.sofaconventions.org>

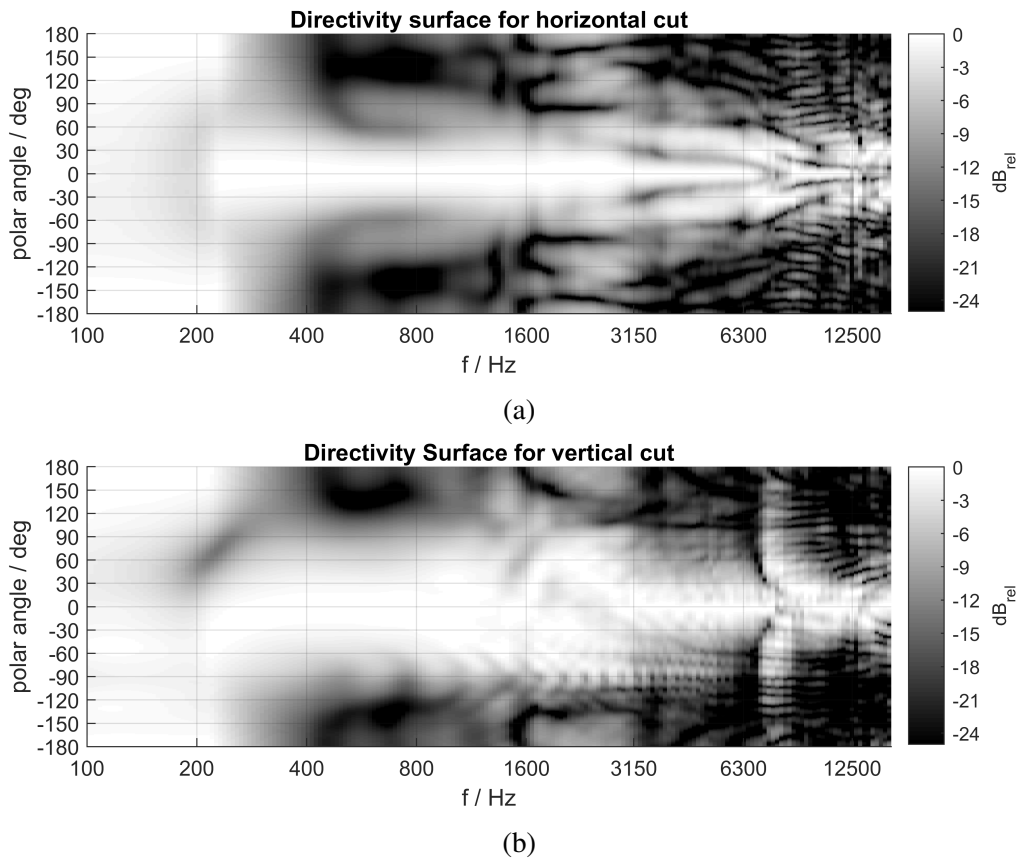


Figure 11 – 170 protot: Directivity surface for a) horizontal and b) vertical cut through the relative sound pressure over frequency and polar angle for a beam pointed at the first horizontal loudspeaker $\theta_{beam} = [52^\circ 90^\circ]^T$.

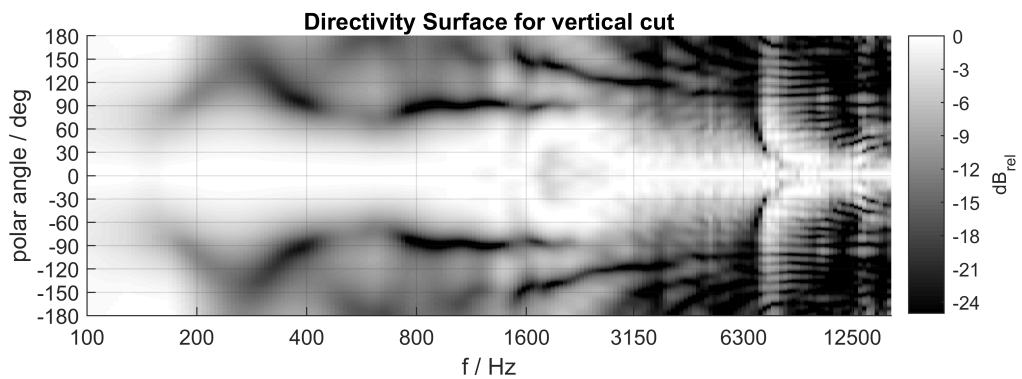


Figure 12 – 171 simulation: Directivity surface for vertical cut through the relative sound pressure over frequency and polar angle for a beam pointed at the first horizontal loudspeaker $\theta_{beam} = [52^\circ 90^\circ]^T$.

5 Simulating a 171 design

With the 170 design, it is possible to control the seven degrees of freedom of the third order on the horizon which enables horizontal 3rd-order ambisonics panning. However, the vertical beamforming behavior is limited. If the focus is kept not so much on enabling elevated beamforming but on narrowing the vertical beam width, a clever approach is to add a second vertical loudspeaker on the opposite side. With this done, an additional spherical harmonic can be utilized for the mixed order beamforming. This is achieved by driving the groups of the two vertical and the seven horizontal speakers with inverse phase, giving the spherical harmonic of second order and zeroth degree Y_2^0 . Since we are interested in making the horizontal beam width more narrow, the spherical harmonics Y_1^0 and Y_2^0 can be driven with opposite phase to yield cancellation near the two poles and additive superposition on the horizon. The spherical harmonic Y_2^0 allows jointly control of the two vertical speakers which allows to stay with the more practical 8-channel control.

We used the directivity measurement from the 170 prototype and mirrored it with regards to the horizon to allow predictions on the effectiveness of a 171 design. This and the control filters updated with the new mixed-order beamforming were used as simulation data to be fed into the analyzing tool to plot a directivity map, cf. Figure 12.

Comparing the result with the 170 prototype, a substantial improvement in focus is observed for frequencies from 400 Hz to 3 kHz (polar angle of $\pm 60^\circ$ vs. $\pm 90^\circ$). Again, the beam pattern is disturbed by spatial aliasing and comb filters. However, the simulation does not show ripple introduced by floor reflections as much, which is due to the simulation method that symmetrizes the acoustic scenario with regard to up-down direction.

All in all, the simulation of an opposite loudspeaker shows that adding another spherical harmonic to the control system may yield great benefits in vertical focusing. In practice however, the crosstalk of a real 171 design will differ from the simulation due to different housing geometries and the cross-talk cancellation system would have to be reevaluated for more realistic results. They may not have a big influence on the beamforming capability, but the behavior in an actual acoustic environment and the overall sound quality is only roughly simulated by this simple simulation.

6 Conclusion and Outlook

In this work, a new weatherproof 170 compact spherical loudspeaker array was designed, produced, measured and finalized for operation with control filters and EQs. The prototype built in this project has met the requirements of its client. It was successfully used in an installation at Norges Hjemmefrontmuseum in Oslo for 4 weeks in September until October 2022 without any damages due to environmental influences. To support reproducible research and to enthuse others in their efforts to reproduce the proposed design a documentation is openly accessible. The CAD model, assembly list, control filters, equalizers, velocity measurements and high resolution directivity measurement are accessible via a link⁸ for free usage.

Moreover, an outlook was made by simulating a 171 design that showed first insights on benefits of this design, e.g. better horizontal focusing, and building and measuring a prototype could consolidate and deepen this approach for compact loudspeaker arrays. Geometrical difficulties have to be mastered, since the additional speaker would be mounted where the mounting flange is located in the current 170 design.

8. https://git.iem.at/benedikt_brands/170-loudspeaker-array

References

- [Dan00] J. Daniel, “Représentation de champs acoustiques, application à la transmission et à la reproduction de scènes sonores complexes dans un contexte multimédia,” Ph.D. dissertation, Université Paris 6, 2000.
- [DZB20] V. Drack, F. Zotter, and N. Barrett, “A personal, 3D printable compact spherical loudspeaker array,” in *AES Conv. e-Brief*, June 2020.
- [LV86] S. P. Lipshitz and J. Vanderkooy, “In-phase crossover network design,” *Journal of the Audio Engineering Society*, vol. 34, no. 11, pp. 889–894, November 1986.
- [MKZP18] N. Meyer-Kahlen, F. Zotter, and K. Pollack, “Design and measurement of first-order, horizontally beam-controlling loudspeaker cubes,” in *Audio Engineering Society Convention 144*, May 2018. [Online]. Available: <http://www.aes.org/e-lib/browse.cfm?elib=19559>
- [RZ20] S. Riedel and F. Zotter, “Design, control, and evaluation of mixed-order, compact spherical loudspeaker arrays,” *Computer Music Journal*, vol. 44, no. 4, pp. 60–76, 2020. [Online]. Available: https://doi.org/10.1162/comj_a_00581
- [ZF12] F. Zotter and M. Frank, “All-round ambisonic panning and decoding,” *Journal of the Audio Engineering Society*, vol. 60, no. 10, pp. 807–820, october 2012. [Online]. Available: <https://www.aes.org/e-lib/browse.cfm?elib=16554>
- [ZSH07] F. Zotter, A. Sontacchi, and R. Höldrich, “Modeling a spherical loudspeaker system as multipole source,” in *Fortschritte der Akustik, DAGA*, Stuttgart, March 2007.
- [ZZFK17] F. Zotter, M. Zaunschirm, M. Frank, and M. Kronlachner, “A beamformer to play with wall reflections: The icosahedral loudspeaker,” *Computer Music Journal*, vol. 41, no. 3, pp. 50–68, Sep. 2017. [Online]. Available: https://doi.org/10.1162/comj_a_00429